Indo. J. Chem. Sci. 15 (1) (2026)
Indonesian Journal of Chemical Science
http://journal.unnes.ac.id/sju/index.php/ijcs

Exploring Natural Product Primary Sulfamates as Carbonic Anhydrase II Ligands: A Computational Approach

Rhamal Amir[1], Aden Dhana Rizkita[2], Candra Hermawan[2], Vivi Amalia Dwi Pratiwi[2], Taufik Muhammad Fakih[3], and Sintia Ayu Dewi[4,5]✉

[1]Department of Pharmacy, Faculty of Science, Technology and Health Sciences, Universitas Bina Mandiri Gorontalo, Indonesia
[2]Department of Pharmacy, Sekolah Tinggi Ilmu Kesehatan Bogor Husada, Indonesia
[3]Department of Pharmacy, Faculty of Mathematics and Natural Sciences, Universitas Islam Bandung, Indonesia
[4]Graduate Institute of Pharmacognosy, Collage of Pharmacy, Taipei Medical University, Taipei, Taiwan
[5]Ph.D. Program in Clinical Drug Development of Herbal Medicine, Collage of Pharmacy, Taipei Medical University, Taipei, Taiwan
No.250, Wuxing St., Xinyi Dist., Taipei City 110, Taiwan Tel: 02-2736-1661

Article Info

Accepted: 10-12-2025

Approved: 04-05-2026

Published: 30-05-2026

Keywords:
Carbonic anhydrase II
Natural product primary sulfamates
Molecular docking
ADMET profiling
PASS anticancer prediction

Abstract

Carbonic anhydrase II (CA II) is a validated metalloenzyme target, classically inhibited by primary sulfonamides such as acetazolamide (AZM), but issues with selectivity and physicochemical properties drive the search for alternative zinc-binding scaffolds. Here, seven naturally occurring primary sulfamates and sulfonamides—(−)-altemicidin, psammaplin C, nucleocidin, 5′-O-sulfamoyladenosine, 5′-O-sulfamoyl-2-chloroadenosine, 5′-O-sulfamoyl-2-bromoadenosine, and 5′-O-sulfamoyltubercidin—were evaluated as potential CA II inhibitor scaffolds using an integrated in silico strategy, with AZM as reference. SwissADME analysis showed all derivatives to be within an acceptable small-molecule space, with higher molecular weights (345–425 g/mol) and polarity than AZM (208.22 g/mol), yet comparable TPSA values for psammaplin C, 5′-O-sulfamoyltubercidin, and 5′-O-sulfamoyladenosine (150–197 Å² vs. 151.66 Å²). ADMET predictions indicated uniformly low gastrointestinal absorption, lack of blood–brain barrier permeability, non-substrate behavior for P-glycoprotein, and no CYP450 inhibition. PASS analysis revealed markedly higher predicted anticancer activity for 5′-O-sulfamoyl-2-chloroadenosine, 5′-O-sulfamoyladenosine, and 5′-O-sulfamoyl-2-bromoadenosine (Pa up to 0.927; IAP > 0.89) compared with AZM. Molecular docking showed all derivatives binding CA II at least as well as AZM (−6.7 kcal/mol), with top scores for 5′-O-sulfamoyl-2-chloroadenosine (−8.0 kcal/mol), 5′-O-sulfamoyl-2-bromoadenosine (−7.8 kcal/mol), and 5′-O-sulfamoyltubercidin (−7.7 kcal/mol), supported by extensive hydrogen bonding and hydrophobic contacts. Collectively, these nucleoside-based primary sulfamates emerge as promising natural scaffolds for next-generation CA II-targeted therapeutics.

© 2026 Universitas Negeri Semarang

✉ Correspondence address:
No.250, Wuxing St., Xinyi Dist., Taipei City 110, Taiwan Tel: 02-2736-1661
E-mail: m303112008@tmu.edu.tw

p-ISSN 2252-6951
e-ISSN 2502-6844

Introduction

Carbonic anhydrases (CAs, EC 4.2.1.1) are ubiquitous zinc metalloenzymes that catalyze the reversible hydration of carbon dioxide to bicarbonate and protons, a fundamental reaction in pH regulation, respiration, electrolyte balance, and biosynthetic pathways. In humans, at least 15–16 isoforms (hCA I–XV) with distinct tissue distributions and subcellular localizations have been identified, and their dysregulation has been implicated in glaucoma, epilepsy, edema, obesity, cancer, and infectious diseases (Kumar et al., 2021; Supuran, 2024). Among the cytosolic isoforms, carbonic anhydrase II (CA II) is one of the most abundant and catalytically efficient, serving as a key target in ophthalmology, nephrology, and oncology (Kumar et al., 2021; Shahsuvaryan, 2022).

Clinically used carbonic anhydrase inhibitors (CAIs) such as acetazolamide, methazolamide, dorzolamide, and brinzolamide are predominantly primary sulfonamides that coordinate the active-site Zn^{2+} ion as deprotonated anions, while the remaining "tail" portion of the molecule engages residues shaping the hydrophobic pocket (Supuran, 2019; Supuran, 2020). Sulfamates and sulfamides represent related zinc-binding groups that can bind to the metal center in a comparable fashion and have also reached clinical use (e.g., topiramate, zonisamide) (Supuran, 2019; Supuran, 2013). Despite their success, many sulfonamide-based CAIs exhibit suboptimal isoform selectivity, leading to off-target inhibition and adverse effects such as paresthesia, metabolic acidosis, nephrolithiasis, and taste disturbances (Kumar et al., 2021; Shahsuvaryan, 2022). These limitations have stimulated the search for new chemotypes and alternative zinc-binding motifs that can improve pharmacological profiles and isoform selectivity while retaining potent CA II inhibition.

Natural products remain a powerful source of structurally diverse and biologically privileged scaffolds, (Rizkita et al., 2021) and they have historically contributed to the discovery of many enzyme inhibitors, including CAIs (Poulsen and Davis, 2013). However, natural products bearing *primary* sulfonamide or sulfamate groups are comparatively rare, making them intriguing templates for metalloenzyme inhibitor design (Poulsen and Davis, 2013; Mujumdar et al., 2016). Psammaplin C, a bromotyrosine-derived marine metabolite, is one of the very few described natural primary sulfonamides and displays nanomolar inhibition of tumor-associated CA isoforms, highlighting how natural scaffolds can provide high affinity and isoform-biased binding modes (Peat et al., 2010). Relatedly, natural and semi-synthetic sulfamate-containing nucleosides—such as nucleocidin (4′-fluoro-5′-O-sulfamoyladenosine) and 5′-O-sulfamoyladenosine derivatives—embody rare sulfamate motifs with potent antibiotic or antiparasitic activity, underlining the pharmacological relevance of the sulfamate group in bioactive small molecules (Shuman et al., 1970; Bloch and Coutsogeorgopoulos, 1971; Carvalho and Oliveira, 2017).

Several additional natural or nature-derived sulfonamide/sulfamate scaffolds illustrate the diversity of this chemical space. (−)-Altemicidin is an unusual sulfonamide alkaloid whose biosynthesis intriguingly co-opts NAD as a building block (Han et al., 2022; Inoue Group, 2021). Dealanylascamycin (5′-sulfamoyl-2-chloroadenosine) and related 5′-O-sulfamoyl halogenated adenosine analogues show antiparasitic and antimicrobial activity and are recognized as distinctive purine nucleoside sulfamates (HMDB, 2021; Stepanchikova et al., 2003). Although not all of these natural sulfamates and sulfonamides have been systematically evaluated as CA II inhibitors, their rare zinc-binding motifs and diverse cores render them attractive *reference scaffolds* for the rational design of new CAIs, particularly given the established compatibility of sulfonamide/sulfamate ZBGs with the CA active site (Supuran, 2019; Poulsen and Davis, 2013).

In parallel with advances in natural product chemistry, computer-aided drug design has become an indispensable strategy for exploring CA II inhibitor space. Recent studies have applied virtual screening, pharmacophore modeling, molecular docking, and molecular dynamics to large libraries of sulfonamides and related chemotypes, successfully identifying novel CA II inhibitors with improved predicted potency and selectivity (Julianti et al., 2023; Arunachalam et al., 2025; Pontecorvi et al., 2025). Early-stage ADME and toxicity profiling using in silico tools helps prioritize compounds with favorable physicochemical and pharmacokinetic properties before costly synthesis and biological testing (Kumar et al., 2021; Supuran, 2019). The SwissADME web tool, for example, provides robust prediction of key descriptors (lipophilicity, solubility, permeability, metabolism liabilities, and "drug-likeness") for small molecules and is now widely integrated into hit-to-lead workflows (Daina et al., 2017). Complementarily, the PASS (Prediction of Activity Spectra for Substances) platform uses structure-activity relationships from large training sets to estimate the probability of thousands of biological activities—including mechanisms of action and potential toxicities—based solely on 2D structure, making it a powerful filter for prioritizing bioactive scaffolds (Lagunin et al., 2000; Stepanchikova et al., 2003)

Against this backdrop, naturally occurring sulfonamides and sulfamates represent an underexplored reservoir of potential CA II inhibitor templates. In particular, the rare primary sulfonamide and sulfamate motifs present in (−)-altemicidin, psammaplin C, nucleocidin, 5′-O-sulfamoyladenosine, 5′-O-sulfamoyl-2-chloroadenosine, 5′-O-sulfamoyl-2-bromoadenosine, and 5′-O-sulfamoyltubercidin offer a unique opportunity to probe structure–activity relationships relevant to CA II inhibition and zinc coordination. Building on current advances in silico methods, the present study investigates these seven natural products

and congeners as *reference scaffolds* for CA II inhibition. Through an integrated computational pipeline comprising SwissADME-based physicochemical and pharmacokinetic profiling, additional ADME prediction, PASS-based biological activity estimation, molecular docking into the CA II active site, and detailed interaction visualization, we aim to identify natural scaffolds that combine favorable drug-like properties with promising binding characteristics toward CA II. By highlighting the most pharmacologically and structurally attractive candidates among these rare natural sulfonamides and sulfamates, this work is expected to support the rational design of alternative CA II inhibitors with improved molecular features and therapeutic potential.

Method

Ligand Collection and Preparation

Seven naturals primary sulfamate compounds were selected based on the scientific literature and reconstructed using MarvinSketch/Marvin JS according to their reported structures. Each compound was energy-minimized and converted into a standardized three-dimensional format (.mol2 or .pdb). No structural modifications or synthetic derivative design steps were performed, ensuring that all analyses reflected the native forms of the natural products. (Fakih et al., 2025)

In Silico Predictions (Physicochemical, ADME, and Cell Line Activity)

Lipinski's Rule of Five evaluation was performed using SwissADME to obtain key physicochemical parameters, including molecular weight, hydrogen bond donors and acceptors, rotatable bonds, TPSA, and molar refractivity. These data were used to assess the drug-likeness of the seven natural primary sulfamate compounds. (Suwendar et al., 2025)

ADME predictions were also generated using SwissADME, covering gastrointestinal (GI) absorption, blood–brain barrier (BBB) permeability, skin permeability (Log Kp), P-glycoprotein substrate status, and CYP inhibition (CYP1A2, CYP2C19, CYP2C9, CYP2D6, and CYP3A4). These parameters provided an overview of each compound's pharmacokinetic profile. (Rizkita et al., 2024)

Cell line activity prediction was conducted using the PASS (Way2Drug) server, which generated the probability of activity (Pa), inactivity (Pi), and invariant accuracy of prediction (IAP) across multiple cancer-related cell lines. Compounds with Pa > Pi were considered potentially active. (Fakih et al., 2025)

Protein Preparation

The crystal structure of human Carbonic Anhydrase II (PDB ID: 2H4N) was retrieved from the Protein Data Bank. Protein preparation was carried out in PyMOL, including the removal of crystallographic water molecules, addition of polar hydrogens, correction of incomplete residues, and standardization of protonation states. The finalized protein was exported in. pdbqt format for docking simulations, ensuring that the catalytic zinc ion and surrounding active-site residues remain intact.

Molecular Docking

Docking simulations were performed using PyRx incorporating the AutoDock Vina engine. Each ligand was docked into the CA II active site, and the most energetically favorable binding poses were selected based on the calculated binding affinity (ΔG, kcal/mol). Docking outputs were examined to understand ligand orientation, zinc coordination potential, hydrogen bonding networks, and hydrophobic interactions within the active-site cavity.

Visualization and Superimposition

Visualization and structural analysis were performed using BIOVIA Discovery Studio and PyMOL. Two-dimensional interaction diagrams and ligand–residue contacts were generated in Discovery Studio. Superimposition was conducted in PyMOL using the super function to compare each natural primary sulfamate compound with the reference ligand acetazolamide and to obtain RMSD values. These visual analyses supported the interpretation of structural similarity and potential binding orientations.

Results and Discussion (Select Header Style)

Physicochemical and Druglikeness Properties of Acetazolamide and and 7 Natural Products Primary Sulfamates

The physicochemical properties of acetazolamide and 7 natural product primary sulfamates were evaluated to assess their druglikeness and early oral suitability. Key descriptors, including molecular weight, hydrogen-bond acceptors and donors, rotatable bonds, aromaticity, fraction Csp^3, topological polar surface area (TPSA), and Lipinski's Rule of Five compliance, were calculated using SwissADME. These parameters

provide an initial indication of membrane permeability, solubility, and overall druglikeness. The complete set of physicochemical data for all compounds is presented in Table 1.

Table 1. Physicochemical and Druglikeness Properties of Acetazolamide and 7 Natural Products Primary Sulfamates

Compound	Physicochemical properties									
	Formula	Mw (g/mol)	Num. heavy atoms	Num. arom. heavy atoms	Fraction Csp3	Num. rotatable bonds	Num. H-bond acceptors	Num. H-bond donors	Molar Refractivity	TPSA (Å²)
AZM	$C_3H_4N_4O_3S_2$	208.22 g/mol	12	5	0.00	3	6	2	40.80	151.66
(−)-Altemicidin	$C_{13}H_{19}N_4O_7S$	375.38 g/mol	25	0	0.62	6	8	4	85.32	204.33
Psammaplin C	$C_{11}H_{14}BrN_3O_5S$	380.21 g/mol	21	6	0.27	7	7	4	79.45	150.46
Nucleocidin	$C_{10}H_{13}FN_6O_6S$	364.31 g/mol	24	9	0.50	4	11	4	74.36	197.08
5′-O-Sulfamoyladenosine	$C_{10}H_{14}N_6O_6S$	346.32 g/mol	23	9	0.50	4	10	4	74.27	197.08
5′-O-Sulfamoyl-2-chloroadenosine	$C_{10}H_{13}ClN_6O_6S$	380.76 g/mol	24	9	0.50	4	10	4	79.28	197.08
5′-O-Sulfamoyl-2-bromoadenosine	$C_{10}H_{13}BrN_6O_6S$	425.22 g/mol	24	9	0.50	4	10	4	81.97	197.08
5′-O-Sulfamoyltubercidin	$C_{11}H_{15}N_5O_6S$	345.33 g/mol	23	9	0.45	4	9	4	76.47	184.19

Overall, the physicochemical evaluation showed that all seven natural sulfamate derivatives remained within an acceptable range for small-molecule scaffolds, despite their inherently larger and more polar structures. Their molecular weights (345–425 g/mol) and rotatable bond counts (4–7) were higher than acetazolamide yet still compatible with oral small-molecule characteristics. TPSA values were generally elevated (150–204 Å²), reflecting their dense heteroatom composition; however, this trend remained aligned with the high polarity typical of sulfonamide-based CA inhibitors, including acetazolamide (151.66 Å²).

Among the evaluated derivatives, Psammaplin C, 5′-O-Sulfamoyltubercidin, and 5′-O-Sulfamoyladenosine demonstrated the most favorable physicochemical balance. These compounds possessed relatively moderate molecular weights (345–380 g/mol), controlled hydrogen bond donor/acceptor counts, and limited molecular flexibility (4–7 rotatable bonds), all of which support more predictable conformational behavior within the CAII active site. Their TPSA values (150–197 Å²) remained comparable to acetazolamide, suggesting that despite their larger structural frameworks, they maintain a polarity profile suitable for CAII recognition and potential oral druglikeness.

Compared to acetazolamide, which represents a compact and rigid sulfonamide scaffold with low molecular weight (208.22 g/mol), minimal flexibility, and a high but efficient TPSA of 151.66 Å², the natural sulfamate derivatives display markedly greater structural complexity and polarity. Nevertheless, the three most promising candidates retain key physicochemical characteristics that parallel acetazolamide, including comparable TPSA values and moderate hydrogen-bonding capacity. While their larger molecular sizes may impose slightly reduced passive permeability relative to AZM, their balanced donor–acceptor profiles and manageable conformational flexibility suggest that they could still achieve favorable binding interactions within the CAII catalytic pocket. Thus, although they deviate structurally from acetazolamide, these derivatives preserve the essential physicochemical requirements associated with effective CA inhibition.

ADMET Profiling of Acetazolamide and 7 Natural Products Primary Sulfamates

The ADMET properties of acetazolamide and the seven natural sulfamate derivatives were predicted using SwissADME, focusing on gastrointestinal (GI) absorption, blood–brain barrier (BBB) permeability, P-glycoprotein (P-gp) substrate status, skin permeability (logKp), and cytochrome P450 inhibition. Complete ADMET results for all compounds are summarized in Table 2.

All derivatives demonstrated low GI absorption, consistent with the behavior of acetazolamide, reflecting the high polarity and extensive hydrogen-bonding capacity characteristic of sulfonamide-based structures. None of the compounds were predicted to permeate the BBB, and all were classified as non-substrates of P-gp, suggesting minimal likelihood of efflux-mediated reduction in oral bioavailability. Furthermore, no inhibition was predicted for major CYP450 isoforms (CYP1A2, CYP2C19, CYP2C9, CYP2D6, and CYP3A4), indicating a favorable metabolic safety profile with low risk of drug–drug interactions.

Based on skin permeability (logKp) and P-gp non-substrate behavior, Psammaplin C, 5′-O-sulfamoyl-2-chloroadenosine, and nucleocidin emerged as the most favorable ADMET candidates. These molecules exhibited the least negative logKp values (−8.01 to −9.88 cm/s), closely resembling or approaching acetazolamide (−7.75 cm/s), suggesting superior or comparable passive permeability relative to the parent drug. Their lack of CYP inhibition and consistent non-substrate classification for P-gp further support their potential for acceptable oral absorption and low metabolic liability despite the high polarity inherent to their scaffolds.

Compared to acetazolamide, the natural sulfamate derivatives exhibited broadly similar ADMET characteristics, particularly in terms of gastrointestinal absorption, BBB permeability, and metabolic stability. Like AZM, all derivatives were predicted to have low GI absorption, reflecting their similarly high polarity and extensive hydrogen-bonding potential. None of the compounds showed BBB permeability or P-gp substrate behavior, closely mirroring acetazolamide's restricted central nervous system penetration and non-efflux susceptibility. The absence of CYP450 inhibition across all derivatives also parallels the metabolic profile of acetazolamide, indicating minimal risk for enzyme-mediated interactions.

However, differences were notable in skin permeability values. Acetazolamide displayed a comparatively less negative logKp (−7.75 cm/s), indicative of higher passive permeability relative to the more polar derivatives, whose logKp values ranged from −8.01 to −10.54 cm/s. Among them, Psammaplin C demonstrated the closest permeability profile to AZM (−8.01 cm/s), whereas nucleoside-based derivatives showed substantially lower permeability due to their larger size and higher TPSA. These distinctions suggest that while the derivatives retain the overall ADMET pattern of acetazolamide, their increased structural complexity may impose reduced passive permeability but potentially enhanced metabolic safety.

Table 2. ADMET Profiling of Acetazolamide and 7 Natural Products Primary Sulfamates

Compound	GI Absorption	BBB Permeant	Log kp (cm/s)	P-gp substrate	CYP1A2 inhibitor	CYP2C19 inhibitor	CYP2C9 inhibitor	CYP2D6 inhibitor	CYP3A4 inhibitor
AZM	Low	No	-7.75	No	No	No	No	No	No
(−)-altemicidin	Low	No	-10.22	No	No	No	No	No	No
psammaplin C	Low	No	-8.01	No	No	No	No	No	No
nucleocidin	Low	No	-9.88	No	No	No	No	No	No
5′-O-sulfamoyladenosine	Low	No	-10.54	No	No	No	No	No	No
5′-O-sulfamoyl-2-chloroadenosine	Low	No	-9.68	No	No	No	No	No	No
5′-O-sulfamoyl-2-bromoadenosine	Low	No	-9.90	No	No	No	No	No	No
5′-O-sulfamoyltubercidin	Low	No	-9.98	No	No	No	No	No	No

Prediction Profiles of Acetazolamide and 7 Natural Products Primary Sulfamates

Cell line–based anticancer activity prediction was conducted using the PASS online platform to assess the therapeutic potential of acetazolamide and the seven evaluated natural sulfamate derivatives. The analysis provided key predictive parameters, including the probability of activity (Pa), probability of inactivity (Pi), and integrated activity probability (IAP), across a diverse panel of human cancer cell lines. These included leukemia (CCRF-CEM), colon carcinoma (HCT-116), hepatoma (HepG2-CD81), lymphoma (ATH-8), and additional solid tumour models relevant to proliferative and drug-resistant phenotypes. The complete prediction outputs for all compounds are summarized in Table 3.

Table 3. Prediction Profiles of Acetazolamide and 7 Natural Products Primary Sulfamates

COMPOUND	Cell-line	Description	Tissue/Organ	Type	Pa	Pi	IAP
Acetazolamide	HepG2-CD81	Hepatoblastoma (HepG2) cells expressing CD81	Liver	Hepatoblastoma	0.365	0.033	0.851
	NCI-H1703	Non-Small Cell Lung Cancer	Lung	Carcinoma	0.319	0.043	0.932
	HOS-TE85	Osteosarcoma	Bone	Sarcoma	0.218	0.007	0.844
(−)-Altemicidin	-	-	-	-	-	-	-
	-	-	-	-	-	-	-
	-	-	-	-	-	-	-
Psammaplin C	MONO-MAC-6	Adult acute monocytic leukemia	Blood	Leukemia	0.375	0.164	0.807
	WI-38	Embryonic lung fibroblast	Lung	Normal	0.330	0.005	0.943
	CAPAN-1	Pancreas Adenocarcinoma	Pancreas	Adenocarcinoma	0.297	0.021	0.889
Nucleocidin	ATH-8	HTLV-I-infected human T-cell line	Peripheral blood	Normal	0.888	0.004	0.964
	U-937	Histiocytic lymphoma	Haematopoietic and lymphoid tissue	Lymphoma	0.738	0.003	0.926
	Huh-7	Hepatocellular carcinoma	Liver	Carcinoma	0.682	0.003	0.920
5′-O-Sulfamoyladenosine	ATH-8	HTLV-I-infected human T-cell line	Peripheral blood	Normal	0.907	0.003	0.964
	HCT-116	Colon carcinoma	Colon	Carcinoma	0.892	0.005	0.890
	CCRF-CEM	Childhood T acute lymphoblastic leukemia	Blood	Leukemia	0.694	0.006	0.913
5′-O-Sulfamoyl-2-chloroadenosine	HCT-116	Colon carcinoma	Colon	Carcinoma	0.927	0.005	0.890
	ATH-8	HTLV-I-infected human T-cell line	Peripheral blood	Normal	0.872	0.004	0.964
	EKVX	Non-small cell lung carcinoma	Lung	Carcinoma	0.735	0.006	0.841
5′-O-Sulfamoyl-2-bromoadenosine	CCRF-CEM	Childhood T acute lymphoblastic leukemia	Blood	Leukemia	0.925	0.004	0.913
	ATH-8	HTLV-I-infected human T-cell line	Peripheral blood	Normal	0.872	0.004	0.964

COMPOUND	Cell-line	Description	Tissue/Organ	Type	Pa	Pi	IAP
5′-O-Sulfamoyltubercidin	HCT-116	Colon carcinoma	Colon	Carcinoma	0.611	0.018	0.890
	HCT-116	Colon carcinoma	Colon	Carcinoma	0.893	0.005	0.890
	ATH-8	HTLV-I-infected human T-cell line	Peripheral blood	Normal	0.763	0.010	0.964
	DU-145	Prostate carcinoma	Prostate	Carcinoma	0.694	0.008	0.896

Across the evaluated panel, the majority of sulfamate derivatives demonstrated markedly improved predicted anticancer profiles compared with acetazolamide (Pa = 0.365; IAP = 0.851). Among the series, three compounds 5′-O-sulfamoyl-2-chloroadenosine, 5′-O-sulfamoyladenosine, and 5′-O-sulfamoyl-2-bromoadenosine exhibited the highest activities, with consistently elevated Pa values (0.927, 0.907, and 0.925, respectively) and strong IAP scores (>0.89). These derivatives showed predicted activity across several aggressive tumor cell lines, including colon carcinoma (HCT-116), leukemia (CCRF-CEM), and lymphoma (ATH-8), indicating a substantially broader anticancer spectrum than the parent drug. Their enhanced probabilistic profiles suggest that the nucleoside-based sulfamoyl scaffold, along with strategic halogen substitution, may strengthen biological activity and improve target engagement at key anticancer pathways.

Overall, these findings highlight that several of the designed derivatives possess significantly stronger predicted anticancer potential compared with acetazolamide, supporting their prioritization for subsequent docking, interaction analysis, and mechanistic evaluation.

Molecular Docking

Table 4. Docking Results of Acetazolamide and 7 Natural Products Primary Sulfamates

Compound	DG (kcal/mol)	Amino acid residue Hydrogen bond	Hydrophobic	Other
AZM	-6.7	ASN62; ASN67; ASN94; THR199; THR200		
(−)-Altemicidin	-7.2	ASN94; THR199; THR200; RO201; LEU198		
Psammaplin C	-7.3	ASN62; GLN92; THR199; HR200	VAL121	
Nucleocidin	-7.2	ASN94; THR199; THR200		
5′-O-Sulfamoyladenosine	-7.5	ASN62; ASN67; ASN94; THR199; THR200		
5′-O-Sulfamoyl-2-chloroadenosine	-8.0	ASN62; ASN67; ASN94; THR199; THR200	LEU198	
5′-O-Sulfamoyl-2-bromoadenosine	-7.8	ASN62; THR199; THR200	LEU198; AL121; PHE131	
5′-O-Sulfamoyltubercidin	-7.7	GLN92; THR199; THR200		

Molecular docking was carried out to assess the binding affinity and interaction patterns of acetazolamide and the seven natural sulfamate derivatives toward carbonic anhydrase II (CA II). Docking scores were used as indicators of predicted binding strength, with more negative values implying stronger and more favorable interactions within the active site. Acetazolamide produced a docking score of −6.7 kcal/mol, serving as the reference for evaluating the binding performance of the sulfamate analogues. The complete docking results, including interaction residues and interaction types, are summarized in Table 4.

Across the evaluated compounds, all derivatives demonstrated docking scores equal to or more favorable than acetazolamide, indicating that the structural modifications introduced into the natural sulfamate scaffolds did not compromise their binding potential. Several derivatives exhibited markedly enhanced binding energies, particularly 5′-O-sulfamoyl-2-chloroadenosine (−8.0 kcal/mol), 5′-O-sulfamoyl-2-bromoadenosine (−7.8 kcal/mol), and 5′-O-sulfamoyltubercidin (−7.7 kcal/mol), suggesting stronger predicted interactions within the catalytic pocket. These compounds formed extensive hydrogen-bonding networks with key residues such as ASN62, ASN67, ASN94, THR199, and THR200, and in some cases

engaged additional hydrophobic residues (e.g., LEU198, VAL121, PHE131), which likely contribute to their enhanced binding stability. The improved docking scores imply that specific substitutions—such as halogenation or nucleoside-linked sulfamoyl groups—enhance complementarity toward the CA II active site and may facilitate more effective zinc-proximal interactions.

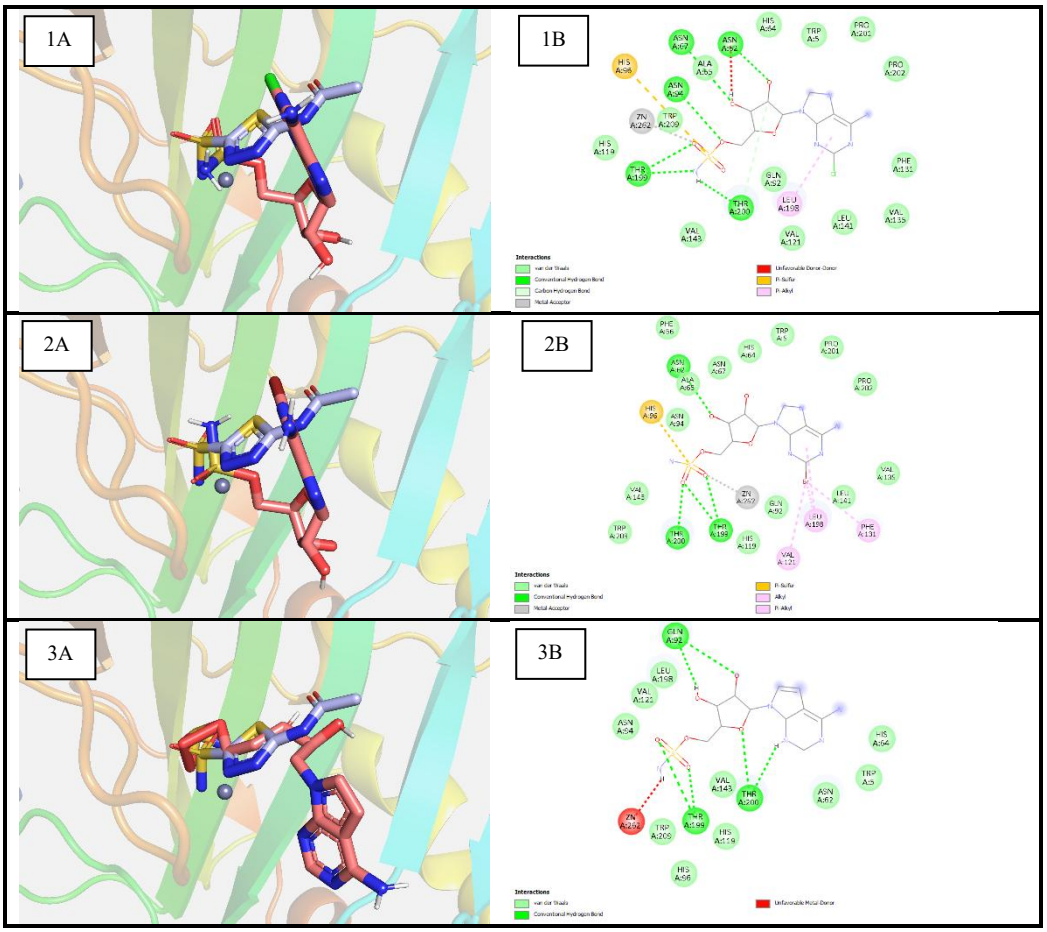

Figure 1. Interpretation of Molecular Docking for Top-3 Compounds Against Human Carbonic Anhydrase II. (1A) Superimpose 5′-O-sulfamoyl-2-chloroadenosine, (1B) 2D structure 5′-O-sulfamoyl-2-chloroadenosine, (2A) Superimpose 5′-O-sulfamoyl-2-bromoadenosine, (2B) 2D structure 5′-O-sulfamoyl-2-bromoadenosine, (3A) Superimpose 5′-O-sulfamoyltubercidin, (3B) 2D structure 5′-O-sulfamoyltubercidin

Among all evaluated derivatives, 5′-O-sulfamoyl-2-chloroadenosine, 5′-O-sulfamoyl-2-bromoadenosine, and 5′-O-sulfamoyltubercidin demonstrated the strongest predicted binding affinities, with docking scores of −8.0, −7.8, and −7.7 kcal/mol, respectively, all of which surpassed acetazolamide (−6.7 kcal/mol). The chlorinated analogue showed the greatest enhancement in affinity, likely attributed to the electron-withdrawing chlorine substituent that increases dipolar interactions and reinforces hydrophobic packing around LEU198 within the CA II pocket. The brominated derivative similarly benefited from a larger, more polarizable halogen atom that enhances van der Waals interactions with hydrophobic residues such as LEU198 and PHE131. Meanwhile, 5′-O-sulfamoyltubercidin displayed improved stabilization through its extended nucleoside scaffold, which enables additional hydrogen bonding with GLN92 and THR199 while maintaining optimal zinc-proximal interactions. Collectively, these results indicate that halogenation and nucleoside-based structural extension significantly enhance ligand complementarity within the CA II active site.

Compared to acetazolamide, the top-performing derivatives exhibited substantial improvements of 1.0–1.3 kcal/mol in docking scores, suggesting that the introduced structural modifications not only preserve the classical sulfonamide zinc-binding orientation but also optimize secondary interactions across adjacent hydrophobic and hydrogen-bonding subpockets. While acetazolamide interacts mainly through its compact heterocyclic core, the best-scoring analogues further exploit peripheral regions of the CA II pocket via halogen-enhanced hydrophobic contacts and additional polar anchoring residues. These enhancements

imply that the designed derivatives may achieve stronger and more stable binding than the reference drug, supporting their potential development as improved CA II inhibitors

Conclusion (Select Header Style)

This study employed a combined physicochemical, ADMET, PASS-based activity, and molecular docking strategy to evaluate seven natural products primary sulfamates and sulfonamides as alternative scaffolds to acetazolamide for CA II inhibition. Despite their larger size and higher polarity, all derivatives remained within an acceptable physicochemical space for small-molecule drug candidates. Psammaplin C, 5′-O-sulfamoyltubercidin, and 5′-O-sulfamoyladenosine exhibited particularly favorable profiles, balancing molecular weight, hydrogen-bonding capacity, and rotatable bond count while maintaining TPSA values comparable to AZM. These characteristics suggest that the natural scaffolds can preserve key features required for CA II recognition while offering increased structural diversity relative to classical sulfonamide inhibitors.

ADMET predictions further indicated that the natural sulfamate derivatives share a broadly similar biopharmaceutical profile with acetazolamide, including low gastrointestinal absorption, lack of blood–brain barrier penetration, non-substrate classification for P-gp, and absence of CYP450 inhibition. Although their higher polarity is associated with slightly reduced passive permeability (more negative logKp values), several compounds—notably psammaplin C, 5′-O-sulfamoyl-2-chloroadenosine, and nucleocidin—displayed permeability parameters close to those of AZM, suggesting that acceptable exposure may still be achievable. Importantly, PASS-based prediction identified 5′-O-sulfamoyl-2-chloroadenosine, 5′-O-sulfamoyladenosine, and 5′-O-sulfamoyl-2-bromoadenosine as having substantially higher predicted anticancer activity than acetazolamide across multiple leukemia, lymphoma, and colon carcinoma cell lines, underscoring the potential of nucleoside-linked sulfamoyl motifs to interact with relevant anticancer pathways.

Molecular docking studies against CA II provided a structural rationale for these trends. All seven natural sulfamate derivatives displayed docking scores equal to or more favorable than acetazolamide, with the top three ligands—5′-O-sulfamoyl-2-chloroadenosine, 5′-O-sulfamoyl-2-bromoadenosine, and 5′-O-sulfamoyltubercidin—exhibiting improvements of approximately 1.0–1.3 kcal/mol in binding energy. These compounds preserved the classical zinc-proximal interaction pattern while expanding hydrogen-bonding and hydrophobic contacts into adjacent subpockets via halogen substitution and nucleoside extension. Such enhanced complementarity suggests the potential for stronger and more stable CA II binding compared with the reference drug.

Taken together, the integrated in silico data support the conclusion that natural product–derived primary sulfamates, particularly halogenated sulfamoyladenosines and 5′-O-sulfamoyltubercidin, represent promising CA II inhibitor scaffolds with improved predicted binding affinity and notable anticancer potential. While these findings are predictive and require experimental confirmation, they provide a rational basis for further structure–activity relationship exploration, synthesis of focused analogues, and subsequent enzymatic and cell-based validation toward the development of next-generation CA II-targeted therapeutics.

Acknowledgments

The authors gratefully acknowledge the support and facilities provided by their home institution during the completion of this work. The authors also thank the developers of SwissADME and PASS Online for providing free, accessible platforms that enabled the physicochemical, ADMET, and activity predictions performed in this study.

References

Arunachalam, S., Balamurali, M. M., & Gnanasekaran, R. (2025). Computational insights into novel inhibitors: virtual screening of small molecules against human carbonic anhydrase II. *Frontiers in Chemistry*, 13, 1627793.

Barra, L., Awakawa, T., Shirai, K., Hu, Z., Bashiri, G., & Abe, I. (2021). β-NAD as a building block in natural product biosynthesis. *Nature*, 600, 747–751.

Bloch, A., & Coutsogeorgopoulos, C. (1971). Inhibition of protein synthesis by 5′-sulfamoyladenosine. *Biochemistry*, 10(22), 4160–4165.

Carvalho, M. F., & Oliveira, R. S. (2017). Natural production of fluorinated compounds and biotechnological prospects of the fluorinase enzyme. *Critical Reviews in Biotechnology*, 37(7), 880–897.

Daina, A., Michielin, O., & Zoete, V. (2017). SwissADME: A free web tool to evaluate pharmacokinetics, drug-likeness and medicinal chemistry friendliness of small molecules. *Scientific Reports*, 7, 42717.

Fakih, T.M., Rizkita, A.D., Dewi, S.A., Muchtaridi, M. In silico approaches for developing sesquiterpene derivatives as antagonists of human nicotinic acetylcholine receptors (nAChRs) for nicotine addiction treatment, Current Research in Structural Biology, Volume 9, 2025, 100162, ISSN 2665-928X, https://doi.org/10.1016/j.crstbi.2024.100162

Fakih, T. M., Darusman, F., Apriliani, R., Prahayati, S., Ramadhan, D. S. F., Fikri Hidayat, A., … Yuniarta, T. A. (2025). Predicting anti-COVID-19 potential: in silico analysis of Mauritine compound from Ziziphus-spina christi as a promising papain-like protease (PLpro) inhibitor. *Journal of Biomolecular Structure and Dynamics*, *43*(14), 7673–7684. https://doi.org/10.1080/07391102.2024.2322627

Human Metabolome Database (HMDB). (2021). Metabocard for 5′-sulfamoyl-2-chloroadenosine (dealanylascamycin, HMDB0248477).

Julianti, N., Firmansyah, A., Amir, R., Rizkita, A. D., & Dewi, S. A. (2023). Effect Of The Extraction Methods On The Identification Of Caffeine In The Extract Of Dragon Fruit Peel. *Indonesian Journal of Chemical Science*, *12*(3), 278-287.

Kende, A. S. (1995). Total synthesis of (−)-altemicidin: A novel exploitation of the Potier–Polonovski rearrangement. *Journal of the American Chemical Society*, 117, 10597–10598.

Kumar, S., Singh, J., Kaur, H., & Kumar, A. (2020). Recent advances in the medicinal chemistry of carbonic anhydrase inhibitors. *European Journal of Medicinal Chemistry*, 207, 112923.

Lagunin, A., Stepanchikova, A., Filimonov, D., & Poroikov, V. (2000). PASS: Prediction of activity spectra for biologically active substances. *Bioinformatics*, 16(8), 747–748.

Maimone, T. J., et al. (2023). Total synthesis of altemicidin: A surprise ending for a monoterpene alkaloid. *JACS Au*, 3, 2883–2893.

Mujumdar, P., & Poulsen, S.-A. (2015). Natural product primary sulfonamides and primary sulfamates. *Journal of Natural Products*, 78(6), 1470–1477.

Mujumdar, P., Teruya, K., Tonissen, K. F., Vullo, D., Supuran, C. T., Peat, T. S., & Poulsen, S.-A. (2016). An unusual natural product primary sulfonamide: Synthesis, carbonic anhydrase inhibition, and protein X-ray structures of psammaplin C. *Journal of Medicinal Chemistry*, 59(7), 3073–3084.

Peat, T. S., et al. (2016). An unusual natural product primary sulfonamide: Synthesis, carbonic anhydrase inhibition, and protein X-ray structures of psammaplin C. *Journal of Medicinal Chemistry*, 59(7), 3073–3084. (same work as above; include only once if your style requires).

Pontecorvi, V., Mori, M., Picarazzi, F., Zara, S., Carradori, S., Cataldi, A., Angeli, A., Berrino, E., Chimenti, P., Ciogli, A., Secci, D., Guglielmi, P., & Supuran, C. T. (2022). Novel insights on human carbonic anhydrase inhibitors based on coumalic acid: Design, synthesis, molecular modeling investigation, and biological studies. *International Journal of Molecular Sciences*, 23(14), 7950.

Poulsen, S.-A., & Davis, R. A. (2014). Natural products that inhibit carbonic anhydrase. In *Natural Products and Cancer Drug Discovery* (Subcellular Biochemistry, Vol. 75, pp. 325–347). Springer.

Rizkita, A. D., Dewi, S. A., Fakih, T. M., & Lee, C. (2024). Effectiveness of sesquiterpene derivatives from Cinnamomum genus in nicotine replacement therapy through blocking acetylcholine nicotinate: a computational analysis. *Journal of Biomolecular Structure and Dynamics*, *43*(9), 4770–4783. https://doi.org/10.1080/07391102.2024.2305315

Rizkita, A. D., Dewi, S. A., Wibowo, E. A. P., & Maulana, I. (2021). Isolation and Identification of Saponins from Leunca Extract (Solanium ningrum L) by Infrared Spectrophotometry. *Scientific Journal Of Science*, *21*(2), 166-169.

Shahsuvaryan, M. L. (2022). Carbonic anhydrase inhibitors in the management of macular edema: A review of the literature. *Medical Hypothesis, Discovery and Innovation in Ophthalmology*, 11(1), 33–41.

Shuman, D. A., Robins, M. J., & Robins, R. K. (1970). Synthesis of nucleoside sulfamates related to nucleocidin. *Journal of the American Chemical Society*, 92(11), 3434–3440.

Supuran, C. T. (2013). Carbonic anhydrases: From biomedical applications of the inhibitors and activators to biotechnological use for CO_2 capture. *Journal of Enzyme Inhibition and Medicinal Chemistry*, 28(2), 229–230.

Supuran, C. T. (2019). Polypharmacology of carbonic anhydrase inhibitors. *Pharmadvances*, 1(Suppl. 1), 3–10.

Supuran, C. T. (2024). Multi- and poly-pharmacology of carbonic anhydrase inhibitors. *Pharmacological Reviews*, 76, e001125.

Suwendar, S., Jantan, I., Fakih, T. M., Priani, S. E., Mulyanti, D., Patricia, V. M., … Rizkita, A. D. (2025). Structural basis for the recognition of anthelmintic activity of bioactive metabolite in watery rose apple leaf through in silico investigation. *Journal of Biomolecular Structure and Dynamics*, *43*(3), 1539–1551. https://doi.org/10.1080/07391102.2023.2292294